

# Binding Energies and Scattering Observables in the ${}^4\text{He}_3$ Atomic System

A. K. Motovilov\*, W. Sandhas

*Physikalisches Institut der Universität Bonn, Endenicher Allee 11-13, D-53115 Bonn, Germany*

S. A. Sofianos

*Physics Department, University of South Africa, P.O.Box 392, Pretoria 0003, South Africa*

E. A. Kolganova

*Joint Institute for Nuclear Research, Dubna, 141980, Russia*

(September 30, 1999)

The  ${}^4\text{He}_3$  bound states and the scattering of a  ${}^4\text{He}$  atom off a  ${}^4\text{He}$  dimer at ultra-low energies are investigated using a hard-core version of the Faddeev differential equations. Various realistic  ${}^4\text{He}$ - ${}^4\text{He}$  interactions were employed, among them the LM2M2 potential by Aziz and Slaman and the recent TTY potential by Tang, Toennies and Yiu. The ground state and the excited (Efimov) state obtained are compared with other results. The scattering lengths and the atom-diatom phase shifts were calculated for center of mass energies up to 2.45 mK. It was found that the LM2M2 and TTY potentials, although of quite different structure, give practically the same bound-state and scattering results.

PACS numbers: 02.60.Nm, 21.45.+v, 34.40.-m, 36.40.+d

## I. INTRODUCTION

Small  ${}^4\text{He}$  clusters (in particular dimers and trimers) are of fundamental interest in various fields of physical chemistry and molecular physics. Studies of these clusters represent an important step towards understanding the properties of helium liquid drops, super-fluidity in  ${}^4\text{He}$  films, the Bose-Einstein condensation *etc.* (see, for instance, Refs. [1–4]). Besides, the helium trimer is probably a unique molecular system where a direct manifestation of the Efimov effect [5] can be observed since the binding energy  $\epsilon_d$  of the  ${}^4\text{He}$  dimer is extremely small.

The  ${}^4\text{He}$  trimer belongs to the three-body systems whose theoretical treatment is quite difficult, first, due to its Efimov nature and, second, because of the hard-core properties of the inter-atomic He–He interaction [6–9]. At the same time the problem of three helium atoms can be considered as an example of an ideal three-body quantum problem since  ${}^4\text{He}$  atoms are identical neutral bosons and, thus, their handling is not complicated by spin, isospin, or Coulomb considerations.

There is a great number of experimental and theoretical studies of  ${}^4\text{He}$  clusters. However, most of the theoretical investigations consist merely in computing the ground-state energy and are based on variational methods [10–15], on Hyperspherical Harmonics expansion methods in configuration space [16,17], and on integral equations in momentum space [18,19]. We further note that the results of Ref. [20] were based on a direct solution of the two-dimensional Faddeev differential equations in configuration space, while recent binding-energy results of [21] were obtained using the three-dimensional Faddeev differential equations in the total-angular-momentum representation.

In Refs. [15,16,19,22] it was pointed out that the excited state of the  ${}^4\text{He}$  trimer is an Efimov state [5]. In these works the HFDHE2 [6], HFD-B [7], and LM2M2 [8] versions of the  ${}^4\text{He}$ - ${}^4\text{He}$  potentials by Aziz and co-workers were employed. The essential property of this state is that it disappears when the inter-atomic potential is increased by a factor  $\lambda \sim 1.2$ . And vice versa, when  $\lambda$  slightly decreases (no more than 2%), a second excited state appears in the trimer [16,19]. It is just such

---

\*On leave of absence from the Joint Institute for Nuclear Research, Dubna, 141980, Russia

a non-standard behavior of the excited-state energies which points at their Efimov nature. The resonance mechanism of formation and disappearance of the Efimov levels in the  ${}^4\text{He}$  trimer has been studied in Refs. [23,24].

The general atom-diatom collision problem has been addressed by various authors, and we refer the interested reader to the review articles [25] and [26]. The collision dynamics at thermal energies of the  $\text{H}+\text{H}_2$  system and the existence of resonances were discussed in [27] using the Faddeev integral equations in momentum space. Finally, the problem of existence of  ${}^4\text{He}$   $n$ -mers and their relation to the Bose-Einstein condensation in  $\text{HeII}$  was discussed in Refs. [28,29]. From the experimental studies we mention those of Refs. [30–35] where molecular clusters, consisting of a small number of noble gas atoms, were investigated.

In contrast to the bulk of theoretical investigations devoted to the binding energies of the  ${}^4\text{He}$  trimer, scattering processes found comparatively little attention. In Ref. [18] the characteristics of the  $\text{He}-\text{He}_2$  scattering at zero energy were studied, while the recombination rate of the reaction  $(1+1+1 \rightarrow 2+1)$  was estimated in [36]. Recently, the phase shifts of the  $\text{He}-\text{He}_2$  elastic scattering and breakup amplitudes at ultra-low energies have also been calculated [22,37,38].

The difficulty in computing excited states and scattering observables in the  ${}^4\text{He}_3$  system is mainly due to two reasons. First, the low energy  $\epsilon_d$  of the dimer makes it necessary to consider very large domains in configuration space with a characteristic size of hundreds of Ångstroems. Second, the strong repulsion of the  $\text{He}-\text{He}$  interaction at short distances produces large numerical errors. In the present paper, which is an extension of our studies for  ${}^4\text{He}_3$  [22–24,37,38], we employed the mathematically rigorous three-body Boundary Condition Model (BCM) of Refs. [39,40] to the above-mentioned problems.

As compared to [22–24,37,38] we employ, in the present work, the refined  $\text{He}-\text{He}$  interatomic potentials LM2M2 by Aziz and Slaman [8], and TTY by Tang, Toennies and Yiu [9]. Our numerical methods have been substantially improved, and this allowed us to use considerably larger grids achieving, thus, a better accuracy. Furthermore, due to much better computing facilities more partial waves could be taken into account.

This paper is organized as follows. In Sec. II we review the three-body bound and scattering state formalism for hard-core interactions. In Sec. III we describe its application to the system of three  ${}^4\text{He}$  atoms and present our numerical results. Our conclusions are summarized in Sec. IV. Finally in the Appendix we give details of the potentials used.

## II. FORMALISM

A detailed analysis of the general boundary-value problem, the derivation of the asymptotic boundary conditions for scattering states and other boundary-value formulations, can be found in Refs. [41,42]. In this work we employ a hard-core version of the BCM [40,43] developed in [39,44] (for details see Ref. [22]). Therefore, in what follows we shall only outline the formalism and present its main characteristics.

In describing the three-body system we use the standard Jacobi coordinates  $\mathbf{x}_\alpha, \mathbf{y}_\alpha$ ,  $\alpha = 1, 2, 3$ , expressed in terms of the position vectors of the particles  $\mathbf{r}_i$  and their masses  $m_i$ ,

$$\mathbf{x}_\alpha = \left[ \frac{2m_\beta m_\gamma}{m_\beta + m_\gamma} \right]^{1/2} (\mathbf{r}_\beta - \mathbf{r}_\gamma)$$

$$\mathbf{y}_\alpha = \left[ \frac{2m_\alpha(m_\beta + m_\gamma)}{m_\alpha + m_\beta + m_\gamma} \right]^{1/2} \left( \mathbf{r}_\alpha - \frac{m_\beta \mathbf{r}_\beta + m_\gamma \mathbf{r}_\gamma}{m_\beta + m_\gamma} \right)$$

where  $(\alpha, \beta, \gamma)$  stands for a cyclic permutation of the indices  $(1, 2, 3)$ .

In the so-called hard-core potential model one requires that the wave function vanishes when the particles approach each other at a certain distance  $r = c$ . This requirement is equivalent to the introduction of an infinitely strong repulsion between the particles at distances  $r \leq c$ . Such a replacement of the repulsive short-range part of the potential by a hard-core interaction turns out to be a very efficient way to suppress inaccuracies at short distances. One can then show that the Faddeev components satisfy the following system of differential equations

$$\begin{cases} (-\Delta_X + V_\alpha - E)\Phi_\alpha(X) = -V_\alpha \sum_{\beta \neq \alpha} \Phi_\beta(X), & |\mathbf{x}_\alpha| > c_\alpha, \\ (-\Delta_X - E)\Phi_\alpha(X) = 0, & |\mathbf{x}_\alpha| < c_\alpha. \end{cases} \quad (1)$$

where  $X \equiv (\mathbf{x}_\alpha, \mathbf{y}_\alpha)$ ,  $\alpha = 1, 2, 3$  and  $c_\alpha$  is the hard-core radius in the channel  $\alpha$ .

Outside the core the components  $\Phi_\alpha$  still provide the total wave function  $\Psi$ ,

$$\Psi(X) = \sum_{\beta=1}^3 \Phi_\beta(X),$$

while in the interior region we have

$$\sum_{\beta=1}^3 \Phi_\beta(X) \equiv 0.$$

In practice, one can replace the latter strong condition by a more weak one [39,44],

$$\sum_{\beta=1}^3 \Phi_\beta(X) \Big|_{|\mathbf{x}_\alpha|=c_\alpha} = 0, \quad \alpha = 1, 2, 3, \quad (2)$$

which requires the sum of  $\Phi_\alpha(X)$  to be zero only at the radius  $c_\alpha$ .

The numerical advantage of our approach is already obvious from the structure of Eqs. (1). When a potential with a strong repulsive core is replaced by the hard-core model, one approximates inside the core domains only the Laplacian  $\Delta_X$  instead of the sum of the Laplacian and the huge repulsive term. In this way a much better numerical approximation can be achieved.

In the present investigation we apply the formalism to the  ${}^4\text{He}$  three-atomic system with total angular momentum  $L = 0$ . The partial-wave version of the equations (1) for a system of three identical bosons with  $L = 0$  reads [45,46]

$$\left[ -\frac{\partial^2}{\partial x^2} - \frac{\partial^2}{\partial y^2} + l(l+1) \left( \frac{1}{x^2} + \frac{1}{y^2} \right) - E \right] \Phi_l(x, y) = \begin{cases} -V(x)\Psi_l(x, y), & x > c \\ 0, & x < c. \end{cases} \quad (3)$$

Here,  $x, y$  are the absolute values of the Jacobi variables and  $c$  is the core size which is the same for all three two-body subsystems. The angular momentum  $l$  corresponds to a dimer subsystem and a complementary atom. For a three-boson system in an  $S$ -state  $l$  can only be even,  $l = 0, 2, 4, \dots$ . The potential  $V(x)$  is assumed to be central and the same for all partial waves  $l$ . The function  $\Psi_l(x, y)$  is related to the partial-wave Faddeev components  $\Phi_l(x, y)$  by

$$\Psi_l(x, y) = \Phi_l(x, y) + \sum_{l'} \int_{-1}^{+1} d\eta h_{ll'}(x, y, \eta) \Phi_{l'}(x', y') \quad (4)$$

where

$$x' = \sqrt{\frac{1}{4}x^2 + \frac{3}{4}y^2 - \frac{\sqrt{3}}{2}xy\eta}, \quad y' = \sqrt{\frac{3}{4}x^2 + \frac{1}{4}y^2 + \frac{\sqrt{3}}{2}xy\eta},$$

with  $\eta = \hat{\mathbf{x}} \cdot \hat{\mathbf{y}}$ . Expressions for the kernels  $h_{ll'}$  can be found in [22,45,46]. It should be noted that these kernels depend only on the hyperangles

$$\theta = \arctan \frac{y}{x} \quad \text{and} \quad \theta' = \arctan \frac{y'}{x'}$$

and not on the hyperradius

$$\rho = \sqrt{x^2 + y^2} = \sqrt{x'^2 + y'^2}.$$

The functions  $\Phi_l(x, y)$  satisfy the boundary conditions

$$\Phi_l(x, y)|_{x=0} = \Phi_l(x, y)|_{y=0} = 0. \quad (5)$$

The partial-wave version of the hard-core boundary condition (2) reads

$$\Phi_l(c, y) + \sum_{l'} \int_{-1}^{+1} d\eta h_{ll'}(c, y, \eta) \Phi_{l'}(x', y') = 0 \quad (6)$$

requiring the wave function  $\Psi_l(x, y)$  to be zero at the core boundary  $x = c$ . Furthermore, one can show that, in general, the condition (6), like the condition (2), causes also the wave functions (4) to vanish inside the core domains. For the bound-state problem one requires that the functions  $\Phi_l(x, y)$  are square integrable in the quadrant  $x \geq 0, y \geq 0$ .

The asymptotic condition for the helium trimer scattering states reads

$$\begin{aligned} \Phi_l(x, y) = & \delta_{l0} \psi_d(x) \exp(i\sqrt{E_t - \epsilon_d} y) [a_0 + o(y^{-1/2})] \\ & + \frac{\exp(i\sqrt{E_t} \rho)}{\sqrt{\rho}} [A_l(\theta) + o(\rho^{-1/2})] \end{aligned} \quad (7)$$

as  $\rho \rightarrow \infty$  and/or  $y \rightarrow \infty$ . Here we use the fact that the helium dimer bound state exists only for  $l = 0$ .  $\epsilon_d$  stands for the dimer energy while  $\psi_d(x)$  denotes the dimer wave function which is assumed to be zero within the core, i.e.,  $\psi_d(x) \equiv 0$  for  $x \leq c$ .

The coefficients  $a_0$  and  $A_l(\theta)$  describe the contributions of the  $(2+1)$  and  $(1+1+1)$  channels to  $\Phi_l$ , respectively. Both the trimer binding energy  $E_t$  and the difference  $E_t - \epsilon_d$  in (7) are negative which means that for any  $\theta$  the function  $\Phi_l(x, y)$  decreases exponentially as  $\rho \rightarrow \infty$ .

The asymptotic boundary condition for the partial-wave Faddeev components of the  $(2+1 \rightarrow 2+1; 1+1+1)$  scattering wave function reads, as  $\rho \rightarrow \infty$  and/or  $y \rightarrow \infty$ ,

$$\begin{aligned} \Phi_l(x, y; p) = & \delta_{l0} \psi_d(x) \{ \sin(py) + \exp(ipy) [a_0(p) + o(y^{-1/2})] \} \\ & + \frac{\exp(i\sqrt{E} \rho)}{\sqrt{\rho}} [A_l(E, \theta) + o(\rho^{-1/2})] \end{aligned} \quad (8)$$

where  $p$  is the relative momentum conjugate to the variable  $y$ ,  $E$  is the scattering energy given by  $E = \epsilon_d + p^2$ , and  $a_0(p)$  is the elastic scattering amplitude. The functions  $A_l(E, \theta)$  provide us for  $E > 0$  with the corresponding partial-wave breakup amplitudes.

The helium-atom helium-dimer scattering length  $\ell_{\text{sc}}$  is given by

$$\ell_{\text{sc}} = -\frac{\sqrt{3}}{2} \lim_{p \rightarrow 0} \frac{a_0(p)}{p}$$

while the  $S$ -state elastic scattering phase shifts  $\delta_0(p)$  are given by

$$\delta_0(p) = \frac{1}{2} \text{Im} \ln S_0(p) \quad (9)$$

where  $S_0(p) = 1 + 2ia_0(p)$  is the  $(2 + 1 \rightarrow 2 + 1)$  partial-wave component of the scattering matrix.

### III. RESULTS

We employed the Faddeev equations (3) and the hard-core boundary condition (6) to calculate the binding energies of the helium trimer and the ultra-low energy phase shifts of the helium atom scattered off the helium diatomic molecule. As He-He interaction we used three versions of the semi-empirical potentials of Aziz and collaborators, namely HFDHE2 [6], HFD-B [7], and the newer version LM2M2 [8]. Further, we employed the latest theoretical He-He potential TTY of Tang et al. [9]. These potentials are given in the Appendix. In our calculations we used the value  $\hbar^2/m = 12.12 \text{ K \AA}^2$ . All the potentials considered produce a weakly bound dimer state. The energy  $\epsilon_d$  of this state together with the He-He atomic scattering length  $\ell_{\text{sc}}^{(2)}$  are given in Table I. It is interesting to note that the latest potentials LM2M2 and TTY give practically the same scattering length  $\ell_{\text{sc}}$  and dimer energy  $\epsilon_d$ .

A detailed description of our numerical method has been given in Ref. [22]. Therefore, we outline here only the main steps of the computational scheme employed to solve the boundary-value problems (3), (5), (6) and (7) or (8). First, we note that the grid for the finite-difference approximation of the polar coordinates  $\rho$  and  $\theta$  is chosen such that the points of intersection of the arcs  $\rho = \rho_i$ ,  $i = 1, 2, \dots, N_\rho$  and the rays  $\theta = \theta_j$ ,  $j = 1, 2, \dots, N_\theta$  with the core boundary  $x = c$  constitute the knots. The value of  $c$  was fixed to be such that any further decrease of it did not appreciably influence the dimer binding energy  $\epsilon_d$  and the energy of the trimer ground state  $E_t^{(0)}$ . In our previous work [22,37,38]  $c$  was chosen as  $0.7 \text{ \AA}$ . In the present work, however, we choose  $c = 1.0 \text{ \AA}$ . This value of  $c$  provides a dimer bound state  $\epsilon_d$  which is stable within six figures and a trimer ground-state energy  $E_t^{(0)}$  stable within three figures. The  $\rho_i$  are chosen according to the formulas

$$\begin{aligned} \rho_i &= \frac{i}{N_c^{(\rho)} + 1} c, & i &= 1, 2, \dots, N_c^{(\rho)}, \\ \rho_{i+N_c^{(\rho)}} &= \sqrt{c^2 + y_i^2}, & i &= 1, 2, \dots, N_\rho - N_c^{(\rho)}, \end{aligned}$$

where  $N_c^{(\rho)}$  stands for the number of arcs inside the domain  $\rho < c$  and

$$y_i = f(\tau_i) \sqrt{\rho_{N_\rho}^2 - c^2}, \quad \tau_i = \frac{i}{N_\rho - N_c^{(\rho)}}.$$

The nonlinear monotonously increasing function  $f(\tau)$ ,  $0 \leq \tau \leq 1$ , satisfying the conditions  $f(0) = 0$  and  $f(1) = 1$ , is chosen according to

$$f(\tau) = \begin{cases} \alpha_0 \tau & , \tau \in [0, \tau_0] \\ \alpha_1 \tau + \tau^\nu & , \tau \in (\tau_0, 1] \end{cases} .$$

The values of  $\alpha_0$ ,  $\alpha_0 \geq 0$ , and  $\alpha_1$ ,  $\alpha_1 \geq 0$ , are determined via  $\tau_0$  and  $\nu$  from the continuity condition for  $f(\tau)$  and its derivative at the point  $\tau_0$ . In the present investigation we took values of  $\tau_0$  within 0.15 and 0.2. The value of the power  $\nu$  depends on the cutoff radius  $\rho_{\max} = \rho_{N_\rho} = 200\text{--}1000 \text{ \AA}$ , its range being within 3.4 and 4 in the present calculations.

The knots  $\theta_j$  at  $j = 1, 2, \dots, N_\rho - N_c^{(\rho)}$  are taken according to  $\theta_j = \text{arctg}(y_j/c)$  with the remaining knots  $\theta_j$ ,  $j = N_\rho - N_c^{(\rho)} + 1, \dots, N_\theta$ , being chosen equidistantly. Such a choice is required by the need of having a higher density of points in the domain where the functions  $\Phi_l(x, y; z)$  change most rapidly, i. e. for small values of  $\rho$  and/or  $x$ . In this work, we used grids of the dimension  $N_\theta = N_\rho = 500\text{--}800$  while the above number  $N_c^{(\rho)}$  and the number  $N_\theta - (N_\rho - N_c^{(\rho)})$  of knots in  $\theta$  lying in the last arc inside the core domain was chosen equal to 2–5.

Since we consider identical bosons only the components  $\Phi_l$  corresponding to even  $l$  differ from zero. Thus, the number of equations to be solved is  $N_e = l_{\max}/2 + 1$  where  $l_{\max}$  is the maximal even partial wave. The finite-difference approximation of the  $N_e$  equations (3) reduces the problem to a system of  $N_e N_\theta N_\rho$  linear algebraic equations. The finite-difference equations corresponding to the arc  $i = N_\rho$  include initially the values of the unknown functions  $\Phi_l(x, y; z)$  from the arc  $i = N_\rho + 1$ . To eliminate them, we express these values through the values of  $\Phi_l(x, y; z)$  on the arcs  $i = N_\rho$  and  $i = N_\rho - 1$  by using the asymptotic formulas (7) or (8) in the manner described in the final part of Appendix A of Ref. [22]. In [22], however, this approach was used for computing the binding energies only while in the present work this method is extended also to the scattering problem. The matrix of the resulting system of equations has a block three-diagonal form. Every block has the dimension  $N_e N_\theta \times N_e N_\theta$  and consists of the coefficients standing at unknown values of the Faddeev components in the grid knots belonging to a certain arc  $\rho = \rho_i$ . The main diagonal of the matrix consists of  $N_\rho$  such blocks.

In this work we solve the block three-diagonal algebraic system on the basis of the matrix sweep method [47]. The use of this method makes it possible to avoid writing the matrix on the hard drive of the computer. Besides, the matrix sweep method reduces the computer time required by almost one order of magnitude as compared to [22,37,38].

Our results for the trimer ground-state energy  $E_t^{(0)}$  as well as the results obtained by other authors are presented in Table II. It should be noted that most of the contribution to the ground-state energy stems from the  $l = 0$  and  $l = 2$  partial components, the latter being slightly more than 30 %, and is approximately the same for all potentials used. The contribution from the  $l = 4$  partial wave is of the order of 3–4 % (cf. [20]).

It is well known that the excited state of the  ${}^4\text{He}$  trimer is an Efimov state [16,19,22–24]. The results obtained for this trimer excited-state energy  $E_t^{(1)}$ , as well as the results found in the literature, are presented in Table III. To illustrate the convergence of our results we show in Table IV the dependence of the energy  $E_t^{(1)}$  on the grid parameters using the TTY potential. It is seen that the  $l = 0$  partial component contributes about 71 % to the excited-state binding energy. The contribution to  $E_t^{(1)}$  from the  $l = 2$  component is about 25–26 % and from  $l = 4$  within 3–4 %. These values are similar to the ones for the ground state.

Apart from the binding energy calculations, we also performed calculations for a helium atom scattered off a helium dimer for  $L = 0$ . For this we used the asymptotic boundary conditions (8). The results of the scattering length of the collision of the He atom on the He dimer obtained for the HFD-B, LM2M2 and TTY potentials are presented in Table V. As compared to [22] the present calculation is essentially improved (the result  $\ell_{\text{sc}} = 145 \pm 5 \text{ \AA}$  for HFD-B with  $l_{\max} = 2$  was obtained in [22] with a much smaller grid). Within the accuracy of our calculations, the scattering lengths provided by the LM2M2 and TTY potentials, like the energies of the excited state, are exactly the

same. This comes as no surprise as the two potentials produce practically the same two-body binding energies and scattering lengths.

The phase shifts results obtained for the HFD-B, LM2M2 and TTY potentials are given in Tables VI, VII, and VIII. For the HFD-B and TTY potentials they are plotted in Fig. 1. Note that for the phase shifts we use the normalization required by the Levinson theorem [48],  $\delta_L(0) - \delta_L(\infty) = n\pi$ , where  $n$  is the number of the trimer bound states.

The incident energies considered were below as well as above the breakup threshold, i. e., for the  $(2+1 \rightarrow 2+1)$  and the  $(2+1 \rightarrow 1+1+1)$  processes. It was found that after transformation to the laboratory system the phases  $\delta_0^{(l_{\max})}$  for the potentials HFD-B, LM2M2 and TTY for different values of  $l_{\max}$  are practically the same, especially those for LM2M2 and TTY. The difference between the phase shifts  $\delta_0^{(2)}$  and  $\delta_0^{(4)}$  is only about 0.5 %.

It is interesting to compare the values obtained for the  $\text{He}-\text{He}_2$  scattering lengths  $\ell_{\text{sc}}$  with the corresponding inverse wave numbers  $\varkappa^{-1}$  for the trimer excited-state energies. The values of  $\varkappa$ ,  $\varkappa = 2\sqrt{(\epsilon_d - E_t^{(1)})/3}$ , where both the  $E_t^{(1)}$  and  $\epsilon_d$  are given in  $\text{\AA}^{-2}$ , are also presented in Table V. It is seen that the values of  $\varkappa$  are about 1.3–1.7 times smaller than the respective  ${}^4\text{He}$ -atom  ${}^4\text{He}$ -dimer scattering lengths. The situation differs completely from the  ${}^4\text{He}$  two-atomic scattering problem where the inverse wave numbers  $(\varkappa^{(2)})^{-1} = |\epsilon_d|^{-1/2}$  are in a rather good agreement with the  ${}^4\text{He}-{}^4\text{He}$  scattering lengths (see Table I). Such significant differences between  $\ell_{\text{sc}}$  and  $\varkappa^{-1}$  in the case of the  ${}^4\text{He}$  three-atomic system can be attributed to the Efimov nature of the excited state of the trimer which implies that the effective range  $r_0$  for the interaction between the  ${}^4\text{He}$  atom and the  ${}^4\text{He}$  dimer is very large as compared to the  ${}^4\text{He}$  diatomic problem.

#### IV. CONCLUSIONS

In this work we employed a formalism which is suitable for three-body calculations with hard-core potentials. The approach is a hard-core variant of the BCM and, unlike some competing methods, is exact and ideally suited for three-body calculations with two-body interactions with a highly repulsive core. Furthermore, the method is feasible not only for bound-states but also for scattering processes. There is, however, a price to be paid for the exact treatment of the system. The inclusion of higher partial waves, beyond  $l_{\max} = 4$ , is hard to be implemented within the computing facilities we have at our disposal.

The results of the ground-state energy of the  ${}^4\text{He}$  trimer obtained for all four realistic  ${}^4\text{He}-{}^4\text{He}$  potentials compare favorably with alternative results in the literature. Furthermore, the successful location of the excited state, interpreted as an Efimov state, clearly demonstrates the reliability of our method in three-body bound state calculations with hard-core potentials. In addition to binding energy calculations, the formalism has been successfully used to calculate scattering lengths and ultra-low-energy phase shifts of the  ${}^4\text{He}$  atom scattered off the  ${}^4\text{He}$  dimer.

In general the hard-core inter-atomic potential together with other characteristics of the system, makes calculations extremely tedious and numerically unstable. This is not the case in our formalism where the hard core is taken into account from the very beginning in a mathematically rigorous way. Thus, the formalism paves the way to study various ultra-cold three-atomic systems, and to calculate important quantities such as the cross-sections, recombination rates, *etc.*

## ACKNOWLEDGMENTS

The authors are grateful to Prof. V. B. Belyaev and Prof. H. Toki for help and assistance in performing the calculations at the supercomputer of the Research Center for Nuclear Physics of the Osaka University, Japan. The authors also would like to thank J. P. Toennies for very interesting discussions stimulating this investigation. Financial support by the Deutsche Forschungsgemeinschaft, the Russian Foundation for Basic Research, and the National Research Foundation of South Africa, is gratefully acknowledged.

## APPENDIX: THE POTENTIALS USED

The general structure of the realistic semi-empirical potentials HFDHE2 [6] and HFD-B [7] developed by Aziz and co-workers is

$$V(x) = \varepsilon V_b(\zeta) \quad (\text{A1})$$

where  $\zeta = x/r_m$  and the term  $V_b(\zeta)$  reads

$$V_b(\zeta) = A \exp(-\alpha\zeta + \beta\zeta^2) - \left[ \frac{C_6}{\zeta^6} + \frac{C_8}{\zeta^8} + \frac{C_{10}}{\zeta^{10}} \right] F(\zeta),$$

$x$  is expressed in the same length units as  $r_m$  (Å in the present case). The function  $F(\zeta)$  is given by

$$F(\zeta) = \begin{cases} \exp[-(D/\zeta - 1)]^2, & \text{if } \zeta \leq D \\ 1, & \text{if } \zeta > D. \end{cases}$$

In addition to the term  $V_b(\zeta)$  the LM2M2 potential [8] includes the “add on” term  $V_a(\zeta)$ ,

$$V(r) = \varepsilon \{V_b(\zeta) + V_a(\zeta)\}, \quad (\text{A2})$$

having the following form:

$$V_a(\zeta) = \begin{cases} A_a \left\{ \sin \left[ \frac{2\pi(\zeta - \zeta_1)}{\zeta_2 - \zeta_1} - \frac{\pi}{2} \right] + 1 \right\}, & \zeta_1 \leq \zeta \leq \zeta_2 \\ 0, & \zeta \notin [\zeta_1, \zeta_2]. \end{cases}$$

The parameters for the HFDHE2, HFD-B and LM2M2 potentials are given in Table IX.

The form of the theoretical He–He potential TTY is taken from [9]. This potential reads

$$V(x) = A [V_{\text{ex}}(x) + V_{\text{disp}}(x)]$$

where  $x$  stands for the distance between  ${}^4\text{He}$  atoms given in atomic length units. (Following [9] in converting the length units we used the factor 1 a.u.= 0.52917 Å.) The function  $V_{\text{ex}}$  has the form

$$V_{\text{ex}}(x) = D x^p \exp(-2\beta x)$$

with  $p = \frac{7}{2\beta} - 1$ , while the function  $V_{\text{disp}}$  reads

$$V_{\text{disp}}(x) = - \sum_{n=3}^N C_{2n} f_{2n}(x) x^{-2n}.$$

The coefficients  $C_{2n}$  are calculated via the recurrency relation

$$C_{2n} = \left( \frac{C_{2n-2}}{C_{2n-4}} \right)^3 C_{2n-6}.$$

At the same time the functions  $f_{2n}$  are given by

$$f_{2n}(x) = 1 - \exp(-bx) \sum_{k=0}^{2n} \frac{(bx)^k}{k!}$$

where

$$b(x) = 2\beta - \left[ \frac{7}{2\beta} - 1 \right] \frac{1}{x}.$$

The parameters of the TTY potential are given in Table X.

- [1] J. P. Toennies and K. Winkelmann, *J. Chem. Phys.* **66**, 3965 (1977).
- [2] M. V. Rama Krishna and K. B. Whaley, *Phys. Rev. Lett.* **64**, 1126 (1990).
- [3] K. K. Lehman and G. Scoles, *Science* **279**, 2065 (1998).
- [4] S. Grebenev, J. P. Toennies, and A. F. Vilesov, *Science* **279**, 2083 (1998).
- [5] V. Efimov, *Nucl. Phys. A* **210**, 157 (1973).
- [6] R. A. Aziz, V. P. S. Nain, J. S. Carley, W. L. Taylor, and G. T. McConville, *J. Chem. Phys.* **79**, 4330 (1979).
- [7] R. A. Aziz, F. R. W. McCourt, and C. C. K. Wong, *Mol. Phys.* **61**, 1487 (1987).
- [8] R. A. Aziz and M. J. Slaman, *J. Chem. Phys.* **94**, 8047 (1991).
- [9] K. T. Tang, J. P. Toennies, and C. L. Yiu, *Phys. Rev. Lett.* **74**, 1546 (1995).
- [10] S. W. Rick, D. L. Lynch, and J. D. Doll, *J. Chem. Phys.* **95**, 3506 (1991).
- [11] V. R. Pandharipande, J. G. Zabolitzky, S. C. Pieper, R. B. Wiringa, and U. Helmbrecht, *Phys. Rev. Lett.*, **50**, 1676 (1983).
- [12] R. N. Barnett and K. B. Whaley, *Phys. Rev. A* **47**, 4082 (1993).
- [13] M. Lewerenz, *J. Chem. Phys.* **106**, 4596 (1997).
- [14] R. Guardiola, M. Portesi, and J. Navarro, "High-quality variational wave functions for small  ${}^4\text{He}$  clusters", LANL E-print physics/9904037.
- [15] T. González-Lezana, J. Rubayo-Soneira, S. Miret-Artés, F. A. Gianturco, G. Delgado-Barrio, and P. Villareal, *Phys. Rev. Lett.* **82**, 1648 (1999).
- [16] B. D. Esry, C. D. Lin, and C. H. Greene, *Phys. Rev. A* **54**, 394 (1996).
- [17] E. Nielsen, D. V. Fedorov, and A. S. Jensen, *J. Phys. B* **31**, 4085 (1998).
- [18] S. Nakaichi-Maeda and T. K. Lim, *Phys. Rev A* **28**, 692 (1983).
- [19] Th. Cornelius and W. Glöckle, *J. Chem. Phys.* **85**, 3906 (1986).
- [20] J. Carbonell, C. Gignoux, and S. P. Merkuriev, *Few-Body Systems* **15**, 15 (1993).
- [21] V. Roudnev and S. Yakovlev, private communication.
- [22] E. A. Kolganova, A. K. Motovilov, and S. A. Sofianos, *J. Phys. B* **31**, 1279 (1998).
- [23] A. K. Motovilov and E. A. Kolganova, *Few-Body Systems Suppl.* **10**, 75 (1999).
- [24] E. A. Kolganova and A. K. Motovilov, *Phys. Atom. Nucl.* **62** No. 7, 1179 (1999) (LANL E-print physics/9808027).
- [25] D. A. Micha, *Nucl. Phys. A* **353**, 309 (1981).
- [26] A. Kuppermann, *Nucl. Phys. A* **353**, 287 (1981).
- [27] Z. C. Kuruoglu and D. A. Micha, *J. Chem. Phys.* **80**, 4262 (1980).
- [28] H. B. Ghassib and G. V. Chester, *J. Chem. Phys.* **82**, 585 (1984).
- [29] N. H. March, *J. Chem. Phys.* **82**, 587 (1984).
- [30] F. Luo, G. C. McBane, G. Kim, C. F. Giese, and W. R. Gentry, *J. Chem. Phys.* **98**, 3564 (1993).
- [31] F. Luo, C. F. Giese, and W. R. Gentry, *J. Chem. Phys.* **104**, 1151 (1996).
- [32] W. Schöllkopf and J. P. Toennies, *Science* **266**, 1345 (1994).
- [33] U. Buck and H. Meyer, *J. Chem. Phys.* **84**, 4854 (1986).
- [34] O. Echt, K. Sattler, and E. Recknagel, *Phys. Rev. Lett.* **47**, 1121 (1981).

- [35] W. Schöllkopf and J. P. Toennies, *J. Chem. Phys.* **104**, 1155 (1996).
- [36] P. O. Fedichev, M. W. Reynolds, and G. V. Shlyapnikov, *Phys. Rev. Lett.* **77**, 2921 (1996).
- [37] E. A. Kolganova, A. K. Motovilov and S. A. Sofianos, *Phys. Rev. A.* **56**, R1686 (1997).
- [38] A. K. Motovilov, S. A. Sofianos, and E. A. Kolganova, *Chem. Phys. Lett.* **275**, 168 (1997).
- [39] S. P. Merkuriev and A. K. Motovilov, *Lett. Math. Phys.* **7**, 497 (1983).
- [40] S. P. Merkuriev, A. K. Motovilov, and S. L. Yakovlev, *Theor. Math. Phys.* **94**, 306 (1993).
- [41] A. K. Motovilov, *Three-body quantum problem in the boundary-condition model* (PhD thesis (in Russian), Leningrad State University, Leningrad, 1984).
- [42] A. A. Kvitsinsky, Yu. A. Kuperin, S. P. Merkuriev, A. K. Motovilov, and S. L. Yakovlev, *Sov. J. Part. Nucl.* **17**, 113 (1986).
- [43] V. N. Efimov and H. Schulz, *Sov. J. Part. Nucl.* **7**, 349 ( 1976).
- [44] A. K. Motovilov, *Vestnik Leningradskogo Universiteta*, **22**, 76 (1983).
- [45] L. D. Faddeev and S. P. Merkuriev, *Quantum scattering theory for several particle systems* (Dordrecht: Kluwer Academic Publishers, 1993).
- [46] S. P. Merkuriev, C. Gignoux, and A. Laverne, *Ann. Phys. (N.Y.)* **99**, 30 (1976).
- [47] A. A. Samarsky: *Theory of difference schemes* (in Russian) (Nauka, Moscow, 1977).
- [48] N. Levinson, K. Dan. *Vidensk. Selsk. Mat. Fys. Medd.* **25**, 9 (1949).

TABLE I. Dimer energies  $\epsilon_d$ , inverse wave lengths  $1/\varkappa^{(2)}$ , and  ${}^4\text{He}-{}^4\text{He}$  scattering lengths  $\ell_{\text{sc}}^{(2)}$  for the potentials used.

Potential	$E_d$ (mK)	$1/\varkappa^{(2)}$ (Å)	$\ell_{\text{sc}}^{(2)}$ (Å)	Potential	$E_d$ (mK)	$1/\varkappa^{(2)}$ (Å)	$\ell_{\text{sc}}^{(2)}$ (Å)
HFDHE2	-0.83012	120.83	124.65	LM2M2	1.30348	96.43	100.23
HFD-B	-1.68541	84.80	88.50	TTY	1.30962	96.20	100.01

 TABLE II. Ground state energy  $E_t^{(0)}$  results for the helium trimer. The (absolute) values of  $E_t^{(0)}$  are given in K. The grid parameters used were:  $N_\theta = N_\rho = 555$ ,  $\tau_0 = 0.2$ ,  $\nu = 3.6$ , and  $\rho_{\text{max}} = 250$  Å.

Potential	Faddeev equations						Variational methods					Adiabatic approaches	
	$l_{\text{max}}$	This work	[20]	[19]	[18]	[21]	[11]	[10]	[12]	[13]	[14]	[16]	[17]
HFDHE2	0	0.084 <sup>a)</sup> 0.0823		0.082	0.092								0.098
	2	0.114 <sup>a)</sup> 0.1124	0.107	0.11									
	4	0.1167				0.1171	0.1173						
HFD-B	0	0.096 <sup>a)</sup> 0.0942	0.096										
	2	0.131 <sup>a)</sup> 0.1277	0.130										
	4	0.1325				0.1330		0.1193	0.133	0.131	0.129		
LM2M2	0	0.0891											0.106
	2	0.1213											0.1252
	4	0.1259				0.126							
TTY	0	0.0890											
	2	0.1212											
	4	0.1258										0.126	

<sup>a)</sup>Results from [22] for a grid with  $N_\theta = N_\rho = 275$  and  $\rho_{\text{max}} = 60$  Å.

 TABLE III. Excited state energy  $E_t^{(1)}$  results for the helium trimer. The (absolute) values of  $E_t^{(1)}$  are given in mK. The grid parameters used were:  $N_\theta = N_\rho = 805$ ,  $\tau_0 = 0.2$ ,  $\nu_0 = 3.6$ , and  $\rho_{\text{max}} = 300$  Å.

Potential	$l_{\text{max}}$	This work	[19]	[18]	[21]	[16]	[17]
HFDHE2	0	1.5 <sup>a)</sup> 1.46		1.46	1.04		1.517
	2	1.7 <sup>a)</sup> 1.65		1.6			
	4	1.67				1.67	
HFD-B	0	2.5 <sup>a)</sup> 2.45					
	2	2.8 <sup>a)</sup> 2.71					
	4	2.74				2.75	
LM2M2	0	2.02					2.118
	2	2.25					
	4	2.28				2.27	2.269
TTY	0	2.02					
	2	2.25					
	4	2.28					

<sup>a)</sup>Results from [22] for a grid with  $N_\theta = N_\rho = 252$  and  $\rho_{\text{max}} = 250$  Å.

TABLE IV. Trimer excited-state energy  $E_t^{(1)}$  (mK) obtained with the TTY potential for various grids.

$l_{\max}$	$N_\theta = N_\rho = 252$	$N_\theta = N_\rho = 502$	$N_\theta = N_\rho = 652$	$N_\theta = N_\rho = 805$	$N_\theta = N_\rho = 1005$
	$\rho_{\max} = 250 \text{ \AA}$	$\rho_{\max} = 300 \text{ \AA}$			
0	-2.108	-2.039	-2.029	-2.024	-2.021
2	-2.348	-2.273	-2.258	-2.253	-2.248

 TABLE V. Estimations for  ${}^4\text{He}$  atom- ${}^4\text{He}$  dimer scattering lengths  $\ell_{\text{sc}}$  and inverse wave numbers  $\varkappa^{-1}$  corresponding to the excited-state energy  $E_t^{(1)}$  for the HFD-B, LM2M2 and TTY potentials. The accuracy for the scattering lengths is within  $\pm 5 \text{ \AA}$ . The grid parameters used for the calculation of  $\ell_{\text{sc}}$  are:  $N_\theta = N_\rho = 502$ ,  $\tau_0 = 0.18$ ,  $\nu = 3.45$  and  $\rho_{\max} = 460 \text{ \AA}$ .

Potential	$l_{\max}$	$\ell_{\text{sc}} (\text{\AA})$	$\varkappa^{-1} (\text{\AA})$	Potential	$l_{\max}$	$\ell_{\text{sc}} (\text{\AA})$	$\varkappa^{-1} (\text{\AA})$
HFD-B	0	170 <sup>a)</sup>	168	LM2M2/TTY	0	168	113
	2	145 <sup>a)</sup>	138		2	134	98
	4	135	93		4	131	96

<sup>a)</sup>Results from [22] for a grid with  $N_\theta = N_\rho = 320$  and  $\rho_{\max} = 400 \text{ \AA}$ .

 TABLE VI. Phase shift  $\delta_0^{(l_{\max})}$  results (in degrees) for the HFD-B potential for various c.m. energies  $E$  (in mK). The grid parameters used are:  $N_\theta = N_\rho = 502$ ,  $\tau_0 = 0.18$ ,  $\nu = 3.45$ , and  $\rho_{\max} = 460 \text{ \AA}$ .

$E$	$\delta_0^{(0)}$	$\delta_0^{(2)}$	$\delta_0^{(4)}$	$E$	$\delta_0^{(0)}$	$\delta_0^{(2)}$	$\delta_0^{(4)}$	$E$	$\delta_0^{(0)}$	$\delta_0^{(2)}$	$\delta_0^{(4)}$
-1.68541	359.9	359.9	359.9	-1.05	299.1	308.2	309.2	0.95	262.4	272.1	273.7
-1.68	352.6	353.9	354.1	-0.8	290.8	300.4	301.5	1.2	260.0	269.6	270.7
-1.65	341.7	345.0	345.4	-0.55	284.4	294.2	295.4	1.45	257.8	267.3	268.4
-1.60	330.8	337.7	338.2	-0.3	279.3	289.3	290.4	1.7	255.9	265.2	266.3
-1.55	326.9	332.8	333.5	-0.05	275.1	285.2	286.3	1.95	254.1	263.4	264.5
-1.50	322.4	329.0	329.8	0.2	271.4	281.3	282.5	2.2	252.5	261.7	262.7
-1.40	315.4	323.0	323.9	0.45	268.1	277.9	279.0	2.45	251.0	260.1	261.1
-1.30	309.9	318.1	319.1	0.7	265.1	274.8	276.0				

 TABLE VII. Phase shift  $\delta_0^{(l_{\max})}$  results for the LM2M2 potential. The units and grid parameters used are the same as in Table VI.

$E$	$\delta_0^{(0)}$	$\delta_0^{(2)}$	$E$	$\delta_0^{(0)}$	$\delta_0^{(2)}$	$E$	$\delta_0^{(0)}$	$\delta_0^{(2)}$
-1.30348	359.8	359.9	-0.8	304.6	313.8	0.95	267.0	276.2
-1.3	354.1	355.3	-0.55	295.2	304.8	1.2	264.1	273.2
-1.25	337.9	342.3	-0.3	287.9	297.7	1.45	261.5	270.6
-1.20	330.5	336.3	-0.05	282.3	292.2	1.7	259.2	268.1
-1.15	325.2	332.0	0.2	277.7	287.4	1.95	257.1	266.0
-1.10	321.1	328.5	0.45	273.7	283.2	2.2	255.3	264.0
-1.05	317.6	325.5	0.7	270.1	279.5	2.45	253.6	262.3

TABLE VIII. Phase shift  $\delta_0^{(l_{\max})}$  results for the TTY potential. The units and grid parameters used are the same as in Table VI.

$E$	$\delta_0^{(0)}$	$\delta_0^{(2)}$	$\delta_0^{(4)}$	$E$	$\delta_0^{(0)}$	$\delta_0^{(2)}$	$\delta_0^{(4)}$	$E$	$\delta_0^{(0)}$	$\delta_0^{(2)}$	$\delta_0^{(4)}$
-1.30961	359.7	359.8	359.8	-0.8	304.3	313.5	314.6	0.95	266.8	276.1	277.2
-1.308	355.9	356.8	356.9	-0.55	295.0	304.6	305.7	1.2	264.0	273.1	274.2
-1.3	350.2	352.1	352.4	-0.3	287.7	297.5	298.7	1.45	261.4	270.5	271.5
-1.25	336.8	341.4	341.9	-0.05	282.0	292.0	293.2	1.7	259.1	268.1	269.1
-1.2	329.7	335.7	336.4	0.2	277.5	287.3	288.4	1.95	257.0	265.9	266.9
-1.10	320.5	328.1	329.0	0.45	273.5	283.1	284.2	2.2	255.0	263.9	265.0
-1.05	317.1	325.1	326.1	0.7	270.0	279.4	280.5	2.45	253.5	262.2	263.2

TABLE IX. The parameters for the  ${}^4\text{He}-{}^4\text{He}$  Aziz and co-workers potentials used.

Parameter	HFDHE2 [6]	HFD-B [7]	LM2M2 [8]
$\varepsilon$ (K)	10.8	10.948	10.97
$r_m$ (Å)	2.9673	2.963	2.9695
$A$	544850.4	184431.01	189635.353
$\alpha$	13.353384	10.43329537	10.70203539
$\beta$	0	-2.27965105	-1.90740649
$C_6$	1.3732412	1.36745214	1.34687065
$C_8$	0.4253785	0.42123807	0.41308398
$C_{10}$	0.178100	0.17473318	0.17060159
$D$	1.241314	1.4826	1.4088
$A_a$	—	—	0.0026
$\zeta_1$	—	—	1.003535949
$\zeta_2$	—	—	1.454790369

TABLE X. The parameters for the  ${}^4\text{He}-{}^4\text{He}$  TTY potential used.

$A$ (K)	315766.2067 <sup>a)</sup>	$C_6$	1.461
$\beta$ $\left(\text{(a.u.)}^{-1}\right)$	1.3443	$C_8$	14.11
$D$	7.449	$C_{10}$	183.5
$N$	12		

<sup>a)</sup>The value of  $A$  was obtained from the data presented in [9] using, for converting the energy units, the factor  $1\text{K} = 3.1669 \times 10^{-6}$  a.u.

$\delta_0$ , degrees

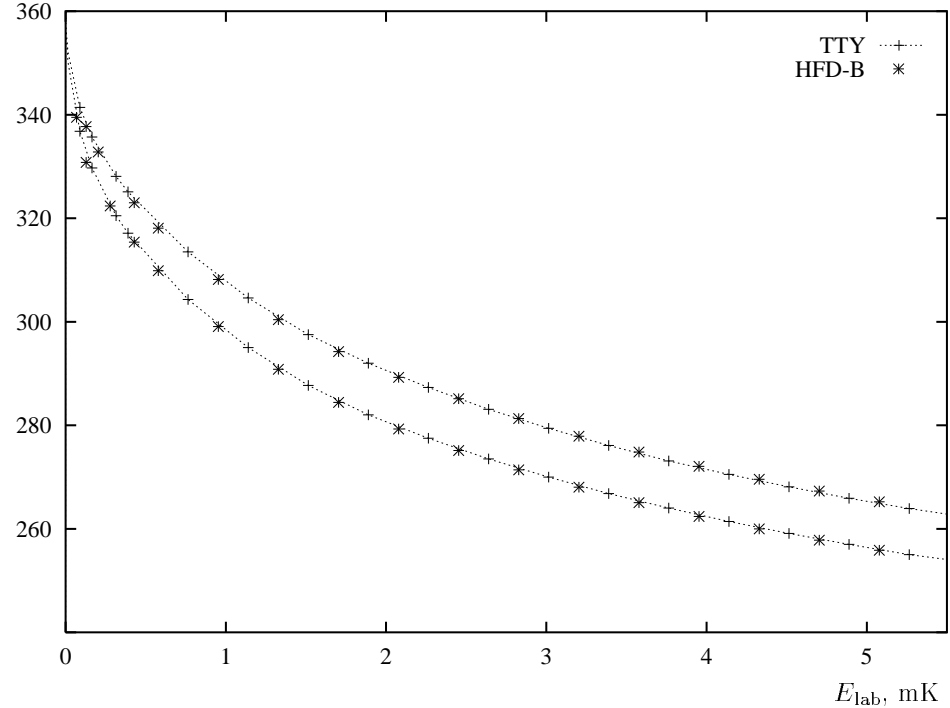


FIG. 1. S-wave helium atom - helium dimer scattering phase shifts  $\delta_0(E_{\text{lab}})$ ,  $E_{\text{lab}} = \frac{3}{2}(E + |\epsilon_d|)$ , for the HFD-B and TTY  ${}^4\text{He} - {}^4\text{He}$  potentials. The lower curve corresponds to the case where  $l_{\text{max}} = 0$  while for the upper  $l_{\text{max}} = 2$ .